European Congress on Computational Methods in Applied Sciences and Engineering
ECCOMAS 2004
P. Neittaanmäki, T. Rossi, S. Korotov, E. Oñate, J. Périaux, and D. Knörzer (eds.)
Jyväskylä, 24–28 July 2004

A MULTISCALE FINITE ELEMENT METHOD

Leopoldo P. Franca*, **Alexandre L. Madureira**†, **and Frederic Valentin**†

*University of Colorado at Denver, P.O. Box 173364, Campus Box 170, Denver, Colorado 80217-3364, USA e-mail: lfranca@math.cudenver.edu, web page:

† LNCC, National Laboratory for Scientific Computation
Av. Getúlio Vargas, 333, 25651-070 Petrópolis, RJ, Brazil e-mails: alm@lncc.br, valentin@lncc.br

Key words: multiscale, singularly perturbed problem, finite element method.

Abstract. *We propose a multiscale finite element method to treat singularly perturbed reaction diffusion equations. We enrich the usual piecewise linear or bilinear finite element trial spaces with local solutions of the original problem, as in the Residual Free Bubble (RFB) setting, but do not require these functions to vanish on each element edge. Such multiscale functions have an analytic expression as long as the data are assumed to be linear. We enrich the space of test functions with bubbles allowing for static condensation, thus our method is of Petrov-Galerkin type. We perform error analysis in different asymptotic regimes and present numerical validations.*

1 INTRODUCTION

It is well known that standard Galerkin method is inadequate to solve singularly perturbed problems. Such limitation is due to the instability of method to approach boundary layers and causes non physical spurious oscillations in the numerical solutions (e.g., see [11] and references therein).

Specially refined meshes, such as Shishkin meshes (see [13] and references therein) can ameliorate this situation. Nonetheless, such strategy become complex when we are confronted to solve problems in complicate geometries, and can be prohibitive to treat realistic three-dimensional problems. Adaptivity is another possibility and consists of associating *a posteriori* estimators to the Galerkin method in order to built refined meshes (see for instance [1] and references therein).

Previous works [5, 8, 9, 14] carried out more stable and accurate formulations based on stabilized methods for the reaction diffusion model, using coarse meshes. The stabilized methods are based on modified variational formulations, but still employ piecewise polynomials. These modifications involve stability parameters, and depend on the residuals of the governing differential equation.

Partial justification of these ideas were made possible by relating stabilized methods to the Galerkin method using piecewise polynomials enriched with "bubble" functions, as illustrated in [2, 3]. To systematically treat various singularly perturbed problems, residual-free bubbles were introduced in [4]. These bubbles are functions with local support which solve, exactly or not, differential equations at the element level, involving the differential operator of the problem. The right hand sides of these local problems are the residuals due to the polynomial part of the solution. The other ingredient is the requirement that the bubble part vanishes on element boundaries for second order problems. Convergence results for linear and bilinear elements can be found in [12]. It turns out that such construction for the reaction diffusion problem yields a poor approximation [6]. Assuming the bubble part of the trial solution to be zero across element edges introduces inaccuracies across element edges.

In this work we have explored a new strategy, without the zero boundary value restriction on each element, conjugate with a Petrov-Galerkin method. We let the test space to be enriched with residual-free bubble functions, but the functions in the trial space have boundary values determined by edge restrictions of the governing differential operator. Such restrictions yield ordinary differential equations that can be solved a priori. Even more importantly, we keep the modification computable at the element level once the data are assumed piecewise linear. Moreover, we develop error estimates for the multiscale finite element method based on [7] proving convergence analysis in two different asymptotic regimes, and we point out sufficient conditions to obtain convergence with respect to the small parameter. We also demonstrate that we recover the standard Galerkin error estimates when the mesh is fine enough.

The paper is organized as follows. In Section 2 we describe our Petrov-Galerkin formulation. In Section 3 we derive error estimates in different asymptotic regimes, and next, in Section 4, we perform numerical tests. Finally in the appendix we present some auxiliary results.

2 THE METHOD

Let Ω be a bounded domain in R^2 with polygonal boundary $\partial\Omega$. We consider $u \in H_0^1(\Omega)$ the weak solution of the reaction diffusion equation

$$\mathcal{L}u := -\varepsilon\Delta u + \sigma u = f \quad \text{in } \Omega, \quad u = 0 \quad \text{on } \partial\Omega, \tag{1}$$

where for simplicity ε and σ are positive constants. We assume f piecewise linear, thus (1) is well-posed.

The usual weak formulation of problem (1) consists on finding $u \in H_0^1(\Omega)$ such that

$$a(u, v) = (f, v), \quad \text{for all } v \text{ in } H_0^1(\Omega), \tag{2}$$

where the bilinear form $a : H_0^1(\Omega) \times H_0^1(\Omega) \to R$ is given by

$$a(u, v) := \varepsilon(\nabla u, \nabla v) + \sigma(u, v). \tag{3}$$

As usual $(\cdot,\cdot)_D$ denotes the inner product in $L^2(D)$ where D is a open subset of Ω. The norm induce by such inner product is denoted by $\|.\|_{0,D}$. To simplify the notation, we write $(\cdot,\cdot)$ and $\|.\|_0$ when $D = \Omega$. The weak problem (2) is well-posed thanks to the coercivity of the bounded bilinear form $a(\cdot,\cdot)$ over $H_0^1(\Omega)$ and the Lax–Milgram Theorem.

Let $\mathcal{T}_h$ be a regular partition of domain Ω into elements K (triangles or quadrangles) with boundary ∂K such that

$$\overline{\Omega} = \bigcup_{K\in\mathcal{T}_h} \overline{K},$$

where the intersection of two elements is either a vertex, or an edge, or empty. We define $\mathcal{V}_h$ as the set of edges Z belonging to $\mathcal{T}_h$, we denote by h_K the characteristic length of $K \in \mathcal{T}_h$, and we set $h = \max_{K\in\mathcal{T}_h}\{h_K\}$. By Ω_{layer}, we denote the set of of elements in $\mathcal{T}_h$ with boundaries that have nontrivial intersection with $\partial\Omega$, and we define

$$\Omega^0 = \Omega\backslash\overline{\Omega}_{layer}, \tag{4}$$

and $h_l = \max_{K\in\Omega_{layer}}\{h_K\}$. In the sequel C, C_1, $C_2, \ldots$ will denote generic positive constants, independent of h_K, ε or σ, but whose value may vary in each occurrence. Moreover, we write $b \simeq d$ meaning that

$$b \le Cd \quad \text{and} \quad d \le Cb. \tag{5}$$

The space $S^1(K)$ will be denoting the space of piecewise linear or bilinear polynomials used to approximate the exact solution. We denote by V_h the standard finite element space

$$V_h := \{v_h \in C^0(\Omega) \,|\, v_{h|_K} \in S^1(K) \text{ for all K} \in \mathcal{T}_h\}, \tag{6}$$

and

$$V_h^0 := V_h \cap H_0^1(\Omega), \tag{7}$$

and the Galerkin scheme associated to the continuous problem reads: *find* $u_g \in V_h^0$ *such that*

$$a(u_g, v_1) = (f, v_1), \quad \text{for all} \quad v_1 \text{ in } \quad V_h^0. \tag{8}$$

It is well known that the Galerkin method (8) is unable to approximate the solution if $\varepsilon \ll \sigma h^2$. To overcome such limitation, we have proposed in [6] a method based on enriching the standard finite element space. The idea is to add special functions, also called multiscale functions, to the usual polynomial spaces to stabilize and improve the accuracy of the Galerkin method. In order to describe the multiscale method, we first need some definitions and notations. We denote by $H_0^1(\mathcal{T}_h)$ and $H^1(\mathcal{T}_h)$ the spaces of functions on Ω whose restriction to each element K belongs to $H_0^1(K)$ and $H^1(K)$, respectively.

Let us introduce the operators $\mathcal{B}_K^i : S^1(\partial K) \to L^2(\partial K)$ defined in the following way: given a basis function q_i of $S^1(\partial K)$ we associate $w_i = \mathcal{B}_K^i q_i \in L^2(\partial K)$ such that

$$\mathcal{L}_{\partial K}^i w_i := -\varepsilon \partial_{ss} w_i + \overline{\sigma}_i w_i = q_i \quad \text{on } \partial K, \quad w_i = 0 \quad \text{at the nodes.} \tag{9}$$

The coefficient $\overline{\sigma}_i$ is set as a positive parameter which can depend on $|K|$ and $|Z|$, and on the node i, where Z denotes an arbitrary edge of ∂K. Such dependence will be specified later (see equation (36)), and we denote by s a variable that parametrize ∂K by arc-length. We point out that (9) is well-posed. A similar boundary condition was used in [10] for elliptic problems with oscillatory coefficients. Now, let $\mathcal{M}_K^i : S^1(K) \to H^1(K)$ be the linear operator defined as follows: given v_i a basis function of $S^1(K)$ let $b_i = \mathcal{M}_K^i\, v_i \in H^1(K)$ be the solution of the problem

$$\mathcal{L} b_i = v_i \quad \text{in } K, \quad b_i = \mathcal{B}_K^i(\frac{\overline{\sigma}_i}{\sigma} v_i) \quad \text{on } \partial K, \tag{10}$$

where $\mathcal{B}_K^i$ are the local operators defined in (9). Since $b_i|_{\partial K}$ belongs to $L^2(\partial K)$ problem (10) is clearly well-posed in each $K \in \mathcal{T}_h$. Therefore, using (10) we introduce the operator $\mathcal{M}_K : S^1(K) \to H^1(K)$ defined by

$$\mathcal{M}_K\, p_h := \sum_i \mathcal{M}_K^i(b_i)\, p_i, \quad p_h \in S^1(K), \tag{11}$$

where p_i represents the coefficients of p_h. Furthermore, we denote by E_h a subspace of $H^1(\mathcal{T}_h)$, called *multiscale space*, such that $E_h \cap V_h^0 = \{0\}$ and defined by

$$E_h := \{v_e \in H^1(\mathcal{T}_h) \,|\, v_{e|_K} = \mathcal{M}_K\, v_1 \text{ for all } v_1 \in V_h\}, \tag{12}$$

where $\mathcal{M}_K$ is the linear operator (10). Hence, an element v_h of $V_h^0 \oplus E_h$ may be uniquely written as

$$v_h := v_1 + v_e,$$

where $v_1 \in V_h^0$ and $v_e \in E_h$. The space E_h is a finite dimensional space and $\dim(E_h) = \dim(V_h)$. We note from (10) that the functions belonging to E_h may be *a priori* discontinuous across the edges of triangles. The continuity is enforced only at the nodes of the triangulation. Therefore, the method is nonconforming. Our approximation of the exact solution in the multiscale space (12) is defined by the solution of the following Petrov-Galerkin problem: *find* $u_h \in V_h^0 \oplus E_h$ *such that*

$$a_h(u_h, v_h) = (f, v_h) \quad \text{for all } v_h \in V_h^0 \oplus H_0^1(\mathcal{T}_h) \tag{13}$$

where

$$a_h(u,v) := \sum_{K \in \mathcal{T}_h} a(u,v)_K,$$

and

$$a(u,v)_K := \varepsilon(\nabla u, \nabla v)_K + \sigma(u,v)_K. \tag{14}$$

From (13) we immediately have that the corresponding $u_h \in V_h^0 \oplus E_h$ satisfies

$$a_h(u_h, v_1) = (f, v_1) \quad \text{for all } v_1 \in V_h^0, \tag{15}$$

$$a(u_h, v_b^K)_K = (f, v_b^K)_K \quad \text{for all } v_b^K \in H_0^1(K). \tag{16}$$

We postpone to Section 3 the discussion of well-posedness of (13). Since by integrating (16) by parts, we have that the enriched part of the solution u_h, denoted by $u_e \in E_h$, is the solution of problem

$$\mathcal{L} u_e = f - \mathcal{L} u_1 \quad \text{in each } K \in \mathcal{T}_h, \tag{17}$$

then, the first equation (15) is immediately satisfied by imposing

$$u_e = \mathcal{M}_K (f - \mathcal{L} u_1). \tag{18}$$

It follows by construction and from (13) that

$$a_h((\mathcal{I} - \mathcal{M}_K \mathcal{L}) u_1, v_1) = (f, v_1) - a_h(\mathcal{M}_K f, v_1) \quad \text{for all } v_1 \in V_h^0, \tag{19}$$

where we have used the relation (18) and $\mathcal{I}$ is the identity operator.

Remark: In the standard enriched strategy with bubble-like functions, as the Residual-Free-Bubble (RFB) approach [4], it is also necessary to solve (17), but assuming that u_e vanishes on all $\partial K \in \mathcal{V}_h$. It turns out that the corresponding local problem must be solved numerically. Unlike the RFB approach, we obtain analytic solutions of (17), thanks to the boundary condition (9) .

Remark: Concerning the stabilized finite element method theory, it is possible to establish analogies between the Residual-Free-Bubble approach and the unusual stabilized method proposed in [8]. This is done by showing that $\mathcal{M}_K = \tau_K \mathcal{I}$ where τ_K is a parameter depending of h_K. We recall that the unusual method reads: *find* $u_1^s \in V_h^0$ *such that*

$$a_s\left(u_1^s, v_1\right) = f_s\left(v_1\right) \quad \text{for all } v_1 \in V_h^0, \tag{20}$$

where the bilinear form $a_s : V_h^0 \times V_h^0 \to R$ reads

$$a_s\left(u, v\right) := a\left(u, v\right) - \sum_{K \in T_h} \left(\tau_K \mathcal{L} u, \sigma v\right)_K \tag{21}$$

and the linear form $f_s : V_h^0 \to R$ is defined by

$$f_s\left(v\right) := \left(f, v\right) - \sum_{K \in T_h} \left(\tau_K f, \sigma v\right)_K . \tag{22}$$

The stabilization parameter τ_K is a piecewise constant function defined by

$$\tau_K = \frac{h_K^2}{\sigma h_K^2 \max\{1, Pe_K\} + 6\varepsilon}, \tag{23}$$

where Pe_K is the Peclet number

$$Pe_K = \frac{6\varepsilon}{\sigma h_K^2}. \tag{24}$$

Concerning the proposed multiscale approach, we believe that it is possible to prove some analogies with the unusual method, but such equivalence in not trivial. This shall be investigated in a future work.

2.1 Corresponding discrete formulation

Let us rewrite (18) in terms of basis functions. We assume that

$$E_h = \text{ span}\{\phi_i\}_{i \in I} \text{ and } \quad V_h = \text{ span}\{\psi_i\}_{i \in I}, \tag{25}$$

where ψ_i are the usual hat functions. Then, f and u_1 are given by

$$u_1 = \sum_{i \in I_0} \psi_i u_i, \quad f = \sum_{j \in I} \psi_j f_j,$$

where u_i , $i \in I_0$, and f_j, $j \in I$, are the nodal values of u and f, respectively. Here I and I_0 are the set of indexes of total and internal nodal points, respectively. It follows from (18), and from the linearity of the operators $\mathcal{L}$ and $\mathcal{L}_{\partial K}^i$ that

$$u_e = \sum_{i \in I_0} \phi_i u_i - \sum_{i \in I} \phi_i \frac{f_i}{\sigma}, \tag{26}$$

where the basis functions $\phi_i \in E_h$, $i \in I$, satisfy

$$\begin{aligned} \mathcal{L}\phi_i &= -\sigma\psi_i \quad \text{in} \quad K, && (27)\\ \phi_i &= \mu_i \quad \text{on } \partial K, && (28) \end{aligned}$$

for all $K \in \mathcal{T}_h$. From (9) and (26), $\mu_i \in L^2(\partial K)$ is the solution of the boundary value problem

$$\mathcal{L}^i_{\partial K}\mu_i = -\overline{\sigma}_i\psi_i \quad \text{in } \partial K \quad \text{and } \mu_i = 0 \quad \text{at the nodes,} \tag{29}$$

on each edge belonging to $\partial K \in \mathcal{V}_h$. It is convenient to present such problem in terms of the unknown $\lambda_i \in V_h^0 \oplus E_h$, $i \in I$, defined by

$$\lambda_j := \psi_j + \phi_j = (\mathcal{I} - \sigma\mathcal{M}_K)\psi_j \quad \text{for all } j \in I. \tag{30}$$

Hence, from the definition (30) the function λ_i, $i \in I$, satisfies

$$\begin{aligned} \mathcal{L}\lambda_i &= 0 \quad \text{in } K, && (31)\\ \lambda_i &= \rho_i \quad \text{on } \partial K, && (32) \end{aligned}$$

where ρ_i, $i \in I$, satisfies the ordinary differential problem

$$\mathcal{L}^i_{\partial K}\rho_i = 0 \quad \text{on } \partial K \quad \text{and } \rho_i = \psi_i \quad \text{at the nodes,} \tag{33}$$

on each edge belonging to $\partial K \in \mathcal{V}_h$.

Thus the discrete version of the weak formulation (19) reads

$$\sum_{j \in I_0} a(\lambda_j, \psi_i) u_j = \sum_{j \in I} \left[a(\lambda_j, \psi_i) - \varepsilon(\nabla\psi_j, \nabla\psi_i)\right] \frac{f_j}{\sigma} \quad \text{for all } i \in I_0. \tag{34}$$

Remark: Numerical experiments indicate that the modified scheme type

$$\sum_{j \in I_0} a(\lambda_j, \psi_i) u_j = \sum_{j \in I} (\lambda_j, \psi_i) \frac{f_j}{\sigma} \quad \text{for all} \quad i \in I_0, \tag{35}$$

yields accurate numerical approximations. This mass lumping trick is, nonetheless, contrary to our general philosophy of deriving the formulation through a sound formalism. Thus, we do not analyse this approach.

2.2 Solving the local problems

Let K be an element of the partition $\mathcal{T}_h$, and Z an edge of its boundary ∂K. First we assume that K is a triangular element. In such case, the dependence of coefficients $\overline{\sigma}_i$ in terms of the shape of elements K is given by

$$\overline{\sigma}_i := \frac{4|K|^2}{|Z|^2|\overline{Z}_i|^2}\sigma, \tag{36}$$

where $\overline{Z}_i$ denotes the corresponding edge of K opposed to the node i. Moreover, we define

$$\gamma_K^i = \left(\frac{\partial \psi_i}{\partial x}|_K\right)^2 + \left(\frac{\partial \psi_i}{\partial y}|_K\right)^2 = \frac{|\overline{Z}_i|^2}{4|K|^2} \simeq h_K^{-2} \quad \text{for all} \quad i \in I, \tag{37}$$

and thanks to the definitions (36), (37) the analytical solution of (31), (32) is given by

$$\lambda_i(x,y) = \frac{\sinh\left(\sqrt{\frac{\sigma}{\gamma_K^i \varepsilon}}\psi_i(x,y)\right)}{\sinh\left(\sqrt{\frac{\sigma}{\gamma_K^i \varepsilon}}\right)} \quad \text{for all} \quad i \in I. \tag{38}$$

Now, we assume that K is a straight quadrangular element, and we chose $\overline{\sigma}_i = 2\sigma$. We observe that the method becomes conform since we impose continuity of shape functions on the boundary ∂K. Without loss of generality, consider a rectangle K with vertexes $1,\ldots,4$ at $(0,0)$, $(h_x,0)$, (h_x,h_y), $(0,h_y)$. Since the bilinear function ψ_1 can be written as $\psi_1(x,y) = \psi_x^1(x)\psi_y^1(y)$, it follows that

$$\lambda_1(x,y) = \frac{\sinh\left(\sqrt{\frac{\sigma}{2\varepsilon}}h_x\psi_x^1(x)\right)\sinh\left(\sqrt{\frac{\sigma}{2\varepsilon}}h_y\psi_y^1(y)\right)}{\sinh\left(\sqrt{\frac{\sigma}{2\varepsilon}}h_x\right)\sinh\left(\sqrt{\frac{\sigma}{2\varepsilon}}h_y\right)}. \tag{39}$$

satisfies (31), (32) exactly. The basis functions λ_j, $j = 2,..4$, are immediately obtained from λ_1 by simply changing variables. By taking a particular node $k \in I$, and look at all elements connected to this node, then the equation (39) illustrate the nodal shape functions λ_k. Fixing $\sigma = 1$, we obtain for $\varepsilon = 1$, 10^{-2}, 10^{-4}, the shape functions λ_k, depicted in Figures 1 and 2. Note that as ε approaches zero, the usual pyramid is squeezed in its domain of influence in the neighborhood around node k. Note that the support of λ_k coincide with the support of the piecewise bilinear function ψ_k.

3 CONVERGENCE RESULTS

We are now concerned with the error analysis of the multiscale method (19) in both ε and h asymptotic limits. We will perform the analysis considering linear interpolation. The bilinear case follows straightforward. For simplicity we perform the error analysis of the method by setting γ_K^i independent of $i \in I$. With such assumption we assume an equilateral triangulation of the domain. The general case is similar, but involves a quite cumbersome symbolic computation (see Lemma 1 below). We start by recalling that the multiscale method (19) reads: *find* $u_1 \in V_h^0$ *such that*

$$a_e(u_1, v_1) = f_e(v_1), \quad \text{for all } v_1 \in V_h^0, \tag{40}$$

where the modified bilinear and linear forms are

$$a_e(u,v) := a(u,v) - a_h(\mathcal{M}_K\mathcal{L}u, v), \quad \text{and} \quad f_e(v) := (f,v) - a_h(\mathcal{M}_K f, v). \tag{41}$$

We first observe that the method (40) is consistent since $\mathcal{M}_K(\mathcal{L}u - f) = 0$, see definition (10). We shall show that the problem (40), and consequently (19), is well-posed. Before presenting the main coercivity result, we need the following estimates.

Lemma 1 *Let the linear operator $\mathcal{M}_K$ be defined by (11). Then, there exist C_λ^1, C_λ^2, C_ρ^1, C_ρ^2, C_θ, C_ξ, C_γ, and C_ζ positive constants only depending on the inner angles of K, and such that for all $v_1 \in V_h$ we have that*

i) $C_\lambda^1 \lambda_{min}^K \|v_1\|_{0,K}^2 \leq ((\mathcal{I} - \sigma\mathcal{M}_K)v_1, v_1)_K \leq C_\lambda^2 \lambda_{max}^K \|v_1\|_{0,K}^2$,

ii) $-C_\rho^1 \rho_{min}^K h_K^{-2} \|v_1\|_{0,K}^2 \leq -(\sigma\nabla\mathcal{M}_K v_1), \nabla v_1)_K \leq 0$,

iii) $0 \leq (\nabla((\mathcal{I} - \sigma\mathcal{M}_K)v_1), \nabla v_1)_K \leq C_\rho^2 \rho_{max}^K h_K^{-2} \|v_1\|_{0,K}^2$,

iv) $\|\mathcal{M}_K v_1\|_{0,K}^2 \leq C_\theta \theta_{max}^K \sigma^{-2} \|v_1\|_{0,K}^2$,

v) $\|\nabla(\mathcal{M}_K v_1)\|_{0,K}^2 \leq C_\xi \xi_{max}^K (\sigma h_K)^{-2} \|v_1\|_{0,K}^2$,

vi) $\|(\mathcal{I} - \sigma\mathcal{M}_K)v_1\|_{0,K}^2 \leq C_\gamma \gamma_{max}^K \|v_1\|_{0,K}^2$,

vii) $\|\nabla((\mathcal{I} - \sigma\mathcal{M}_K)v_1)\|_{0,K}^2 \leq C_\zeta \zeta_{max}^K h_K^{-2} \|v_1\|_{0,K}^2$,

where the quantities constants λ_{min}^K, λ_{max}^K, ρ_{min}^K, ρ_{max}^K, θ_{max}^K, ξ_{max}^K, γ_{max}^K and ζ_{max}^K depend in a nontrivial way on ε, σ, h_K, and are given in the Appendix. Here $h_K = \frac{\gamma_K^i}{C_K}$ where $C_K = 6\frac{C_\rho^1}{C_\lambda^1}$.

Proof: See [7].

We are ready to prove the existence and uniqueness of solution for the problem (40). First, let us consider the local h-dependent norm

$$\|v\|_{E,K} := \sqrt{C_K \alpha_K \|v\|_{0,K}^2 + h_K^2 \|\nabla v\|_{0,K}^2} \quad \text{for all } v \in H^1(\mathcal{T}_h), \tag{42}$$

where α_K is the positive constant given by

$$\alpha_K = \frac{\sigma h_K^2}{C_K \varepsilon} \lambda_{min}^K - \frac{\rho_{min}^K}{6}, \tag{43}$$

and we define $\alpha = \min_{K \in \mathcal{T}_h} \alpha_K$. The positiveness of α_K follows from the definition of eigenvalues ρ_{min}^K and λ_{min}^K. As usual the associate global norm is given by

$$\|v\|_E := \sqrt{\sum_{K \in \mathcal{T}_h} \|v\|_{E,K}^2} \quad \text{for all } v \in H^1(\mathcal{T}_h), \tag{44}$$

and we have the following coercivity result.

Lemma 2 *Let $\|.\|_{E,K}$ be the norm defined by (42). Then, the bilinear form $a_e : V_h \times V_h \to R$ is coercive and*

$$a_e(v_1, v_1) \geq C \sum_{K \in \mathcal{T}_h} \frac{\varepsilon}{h_K^2} \|v_1\|_{E,K}^2 \quad \text{for all } v_1 \in V_h. \tag{45}$$

Proof: The result follows from the definition of bilinear form (41), (43), applying the items (i) and (ii) of Lemma 1, and since $C_K = 6\frac{C_\rho^1}{C_\lambda^1}$.

Remark: Existence and uniqueness of solutions for problem (40) follows from Lax-Milgram Theorem. Let $u_e \in E_h$ be uniquely defined by $u_e = \mathcal{M}_K(f - \sigma u_1)$ in K, where u_1 is the unique solution of (40). Then, $u_e + u_1$ belongs to $V_h^0 \oplus E_h$ and satisfies (13).

Remark: The coefficient presented in the norm definition (42) have the following behavior

$$\lim_{\varepsilon \to 0} \alpha_K = \frac{3}{4} \quad \text{and} \quad \lim_{h_K \to 0} \frac{C_K \varepsilon}{\sigma h_K^2} \alpha_K = \frac{1}{48}. \tag{46}$$

3.1 Convergence with respect to ε

In this case we shall use the asymptotic properties of the exact solution u. As ε goes to zero the exact solution converges, at least away from the boundary, to $f\sigma^{-1}$. We shall estimate the related error in the norm (44), and also bound $u - f\sigma^{-1}$ in the same norm. The final result, i.e., the estimate for $u - u_1$, follows from the triangle inequality. Let us define $\overline{f} \in V_h^0$ such that $\overline{f} = f$ in Ω^0. We have the following estimate.

Lemma 3 *Let u be the solution of (1). Then, there exit C_1, C_2, and C_3 such that*

i) $\left\|u - \frac{f}{\sigma}\right\|_0^2 \leq \frac{C_1}{\sigma^2}\left(h_l \|f\|_{\infty,\Omega^0}^2 + \varepsilon\sigma^{-1}\left\|\nabla\overline{f}\right\|_0^2\right)$,

ii) $\left\|\nabla\left(u - \frac{f}{\sigma}\right)\right\|_0^2 \leq \frac{C_2}{\sigma^2}\left[(h_l\varepsilon^{-1}\sigma + 1)\|f\|_{\infty,\Omega^0}^2 + \left\|\nabla\overline{f}\right\|_0^2\right]$,

iii) $\sum_{K \in \mathcal{T}_h} h_K^2 \left\|\nabla\left(u - \frac{f}{\sigma}\right)\right\|_{0,K}^2 \leq \frac{C_3}{\sigma^2}\left[(h_l^3\varepsilon^{-1}\sigma + h_l^2)\|f\|_{\infty,\Omega^0}^2 + h^2\left\|\nabla\overline{f}\right\|_0^2\right]$.

Proof: See [7].

Corollary 4 *Let u be the solution of (1). Then, there exits constant C such that*

$$\left\|u - \frac{f}{\sigma}\right\|_E \leq \frac{C}{\sigma}\left[h_l^{1/2}\left(h_l\varepsilon^{-1/2}\sigma^{1/2} + 1\right)\|f\|_{\infty,\Omega^0} + \left(h + \varepsilon^{1/2}\sigma^{-1/2}\right)\|\nabla\overline{f}\|_0\right]. \tag{47}$$

Proof: The result follows by the norm definition (42), since $\alpha_K < 1$ for all $K \in \mathcal{T}_h$, and from Lemma 3.

We have the following estimate result.

Lemma 5 *Let u_1 be the solution of (40). There exists C such that*

$$\left\|\frac{f}{\sigma}-u_1\right\|_E \leq \frac{C}{\sigma}\left[h_l\left(h_l^{1/2}\varepsilon^{-1/2}\sigma^{1/2}+1\right)\left(1+\alpha^{-1/2}\right)\|f\|_{\infty,\partial\Omega}+h_l\|\nabla\overline{f}\|_0+h\alpha^{-1/2}\left\|\nabla f\right\|_0\right].$$

Proof: See [7].

We are ready to present the main convergence result.

Theorem 6 *Let u be the solution of (2) and u_1 be the solution of (40). There exists C such that*

$$\|u-u_1\|_E \leq \frac{C}{\sigma}\left\{h_l^{1/2}\left[h_l^{1/2}\left(h_l^{1/2}\varepsilon^{-1/2}\sigma^{1/2}+1\right)\left(1+\alpha^{-1/2}\right)+1\right]\|f\|_{\infty,\partial\Omega}\right.$$
$$\left.+h\alpha^{-1/2}\left\|\nabla f\right\|_0+\left(h+\varepsilon^{1/2}\sigma^{-1/2}\right)\left\|\nabla\overline{f}\right\|_0\right\}.$$

Proof: The result follows using triangle inequality, Corollary 4, Lemma 5, and redefining the constants.

Remark: The convergence result presented in Theorem 6 points out that the error depends on the form of f. Supposing that f vanishes on $\partial\Omega$, then

$$\lim_{\varepsilon\to 0}\|u-u_1\|_E \leq C\frac{h}{\sigma}\left\|\nabla f\right\|_0, \tag{48}$$

since $\alpha \to 3/4$ when $\varepsilon \to 0$. Moreover, if f is supposed to be constant or linear in Ω_0 and $h_l \simeq \varepsilon^p$ with $p \in (0, 1/2]$, thus we have convergence. If f is nonzero on $\partial\Omega$ and $h_l \simeq \varepsilon^p$ with $p \in (1/3, 1/2]$, then

$$\lim_{\varepsilon\to 0}\|u-u_1\|_E \leq C\frac{h}{\sigma}\left(\left\|\nabla f\right\|_0+\left\|\nabla\overline{f}\right\|_0\right), \tag{49}$$

since α is bounded. As long as f is constant or linear in Ω we recover convergence.

3.2 Convergence with respect to h

In this subsection we perform a convergence analysis with respect to h. In what follows, we consider that the positive constant C is independent of h but might depend on ε and σ. First, recall that we denote by u_g the solution of the Galerkin formulation (8). It is well known that there exists constant C such that

$$\sqrt{\sigma}\|u-u_g\|_0+\sqrt{\varepsilon}\|\nabla(u-u_g)\|_0 \leq Ch\|u\|_2. \tag{50}$$

Our first goal consists on estimating the Galerkin error in the norm (44). This is done in the following lemma.

Lemma 7 *Let u be the solution of (2) and u_g be the solution of (8). There exists a constant C such that*

$$\sum_{K \in \mathcal{T}_h} \frac{\sqrt{\varepsilon}}{h_K} \|u - u_g\|_{E,K} \leq Ch\|u\|_2. \tag{51}$$

Proof: The result follows using (44) and (50).

Lemma 8 *Let u_g be the solution of (8) and u_1 be the solution of (40). There exist a constant C such that*

$$\sum_{K \in \mathcal{T}_h} \frac{\sqrt{\varepsilon}}{h_K} \|u_g - u_1\|_{E,K} \leq Ch\|u\|_2. \tag{52}$$

Proof: See [7].

We are ready to present the main convergence result.

Theorem 9 *Let u be the solution of (2) and u_1 be the solution of (40). There exist C such that*

$$\sum_{K \in \mathcal{T}_h} \frac{\sqrt{\varepsilon}}{h_K} \|u - u_1\|_{E,K} \leq Ch\|u\|_2. \tag{53}$$

Proof: The result follows using triangle inequality, and from Lemmas 7 and 8.

Remark: The convergence result (53) is equivalent to the standard Galerkin error in the energy norm.

4 NUMERICAL EXAMPLES

4.1 The unity square: bilinear elements

Let us first consider the unit source problem ($f = 1$) defined on the unit square depicted in Figure 3, subject to a homogeneous boundary condition. For a fixed $\sigma = 1$, and small ε, boundary layers appear close to the domain boundary. Figure 4 shows the solutions of the four different methods described herein, for $\varepsilon = 10^{-6}$. The unusual stabilized method and the current method perform better than the other two methods. Examining the solutions profiles, see Figure 5, it becomes clear that the current method is superior to other methods. For $\varepsilon = 10^{-3}$ and $\varepsilon = 1$, all methods have comparable performance.

4.2 The unity square: linear elements

We consider the discontinuous source problem where f is given by

$$f(x,y) = \begin{cases} 1, & 0 \leq \mathbf{x} < \frac{1}{2}, \\ 0, & \frac{1}{2} \leq \mathbf{x} \leq 1, \end{cases} \tag{54}$$

on the unit square and subject to a homogeneous boundary condition depicted in Figure 6. For a fixed $\sigma = 1$, and small ε, internal and external boundary layers appear. Figure 7 shows the solutions of different methods described herein, including the modified method (35) for $\varepsilon = 10^{-6}$. The current method performs better than the Galerkin method, and it corrects the spurious oscillations. Examining the solutions profiles, see Figure 8, it is interesting to note that the modified method also gives good results close to the internal boundary layer.

5 Appendix

We present in this section the expression of the eigenvalues introduced in Lemma 1, and we show graphically the behavior of some coefficients and eigenvalues. To simplify the formulas, we introduce β_K defined by

$$\beta_K = \sqrt{\frac{\sigma h_K^2}{C_K \varepsilon}}.$$

The expression of eigenvalues are given by

$$\lambda_{min}^K = \frac{1}{\beta_K^2}\left(1 + \frac{3}{\beta_K \sinh\beta_K} - \frac{3\cosh\beta_K}{\beta_K \sinh\beta_K} + \frac{\beta_K}{2\sinh\beta_K}\right),$$

$$\lambda_{max}^K = \frac{1}{\beta_K^2}\left(1 - \frac{\beta_K}{\sinh\beta_K}\right),$$

$$-\rho_{min}^K = -3/2\left(1 + \frac{2}{\beta_K \sinh\beta_K} - \frac{2\cosh\beta_K}{\beta_K \sinh\beta_K}\right),$$

$$\rho_{max}^K = \frac{3}{\beta_K}\left(\frac{\cosh\beta_K}{\sinh\beta_K} - \frac{1}{\sinh\beta_K}\right),$$

$$\gamma_{max}^K = \frac{1}{4\beta_K^2 \sinh(\beta_K)^2}\Big(\cosh(\beta_K)^2 - 8\cosh(\beta_K) - \beta_K^2 + 4\beta\sinh(\beta_K) + 7\Big),$$

$$\zeta_{max}^K = \frac{1}{8\sinh(\beta_K)^2}\Big(2\cosh(\beta_K)^2 - 2\cosh(\beta_K)\sinh(\beta_K) - 1\Big)$$

$$\Big(6\cosh(\beta_K)^4 + 6\cosh(\beta_K)^3\sinh(\beta_K) - 9\cosh(\beta_K)^2 - 6\cosh(\beta_K)\sinh(\beta_K) + 3$$
$$+6{\beta_K}^2\cosh(\beta_K)^2 + 6{\beta_K}^2\sinh(\beta_K)\cosh(\beta_K) - 3{\beta_K}^2$$
$$-\Big(\Big(\cosh(\beta_K)^4 - 2\cosh(\beta_K)^2 + 34{\beta_K}^2\cosh(\beta_K)^2 + 1 - 34{\beta_K}^2 + {\beta_K}^4\Big)$$
$$\Big(1 + 8\cosh(\beta_K)^4 - 8\cosh(\beta_K)^2 + 8\cosh(\beta_K)^3\sinh(\beta_K) - 4\cosh(\beta_K)\sinh(\beta_K)\Big)\Big)^{1/2}\Big),$$

$$\theta_{max}^K = \frac{3}{\beta_K \sinh\beta_K}\left(1 + \frac{-21\,(\cosh\beta_K)^2 - 24\cosh\beta_K - 5{\beta_K}^2 + 45 + 2{\beta_K}^2(\cosh\beta_K)^2}{36\sinh\beta_K\beta_K}\right),$$

$$\xi_{max}^K = \frac{1}{8\,(\beta_K\sinh\beta_K)^2}\Big({\beta_K}^4F(\beta_K) + {\beta_K}^2G(\beta_K) + \beta_K H(\beta_K)\Big),$$

where the functions F, G and H are given by an intricate nonlinear combination of $\sinh\beta_K$ and $\cosh\beta_K$.

REFERENCES

[1] M. Ainsworth and J.T. Oden, *A posteriori error estimation in finite element analyis*. Jonh Wiley and Sons, 2000.

[2] C. Baiocchi and F. Brezzi and L.P. Franca. *Virtual bubbles and the Galerkin-least-squares method*. Computer Methods in Applied Mechanics and Engineering, No. 105, 125–141, 1991.

[3] F. Brezzi and L.P. Franca and T.J.R. Hughes and A. Russo. $b = \int g$. Computer Methods in Applied Mechanics and Engineering, Vol. 145, No. 3–4, 329–339, 1997.

[4] F. Brezzi and A. Russo. *Choosing bubbles for advection-diffusion problems*. Mathematical Models & Methods in Applied Sciences, Vol. 4, No. 4, 571–587, 1994.

[5] L.P. Franca and Eduardo G. Dutra do Carmo. *The Galerkin gradient least-squares method*. Computer Methods in Applied Mechanics and Engineering, Vol. 74, No 1, 41–54, 1989.

[6] L.P. Franca and A.L. Madureira and F. Valentin. *Towards multiscale functions : enriching finite element spaces with local but not bubble-like functions*. Submitted to Computer Methods in Applied Mechanics and Engineering.

[7] L.P. Franca and A.L. Madureira and L. Tobiska and F. Valentin. *Convergence Analysis of a Multiscale Finite Element Method*. Preprint.

[8] L.P. Franca and F. Valentin. *On an improved unusual stabilized finite element method for the advective-reactive-diffusive equation*. Computer Methods in Applied Mechanics and Engineering, Vol. 190, No. 13–14, 1785-1800, 2000.

[9] I. Harari and T.J.R. Hughes. *Stabilized finite elements methods for steady advection-diffusion with production*. Computer Methods in Applied Mechanics and Engineering, Vo. 32, No 115, 165–191, 1994.

[10] T. Y. Hou and X. Wu and Z. Cai. *Convergence of a multiscale finite element method for elliptic problems with rapidly oscillating coefficients*. Math. Comp., Vol. 68, No. 227, 913–943, 1999.

[11] H. Roos and M. Stynes and L. Tobiska. *Numerical methods for singularly pertubed differential equations*. Springer, 1991.

[12] G. Sangalli. *Global and local error analysis for the residual–free bubble method applied to advection–dominated problems*. SIAM J. Numer. Anal, Vol. 38, No. 5, 1496–1522, 2000.

[13] M. Stynes. *A uniform convergent Galerkin method on a Shishkin mesh for a convection diffusion problem.* Journal of Mathematical Analysis and Applications, No. 214, 36–54, 1997.

[14] F. Valentin and L. P. Franca. *Combining Stabilized Finite Element Methods.* Computational and Applied Mathematics, Vol. 14, No 3, 285-300, 1995.

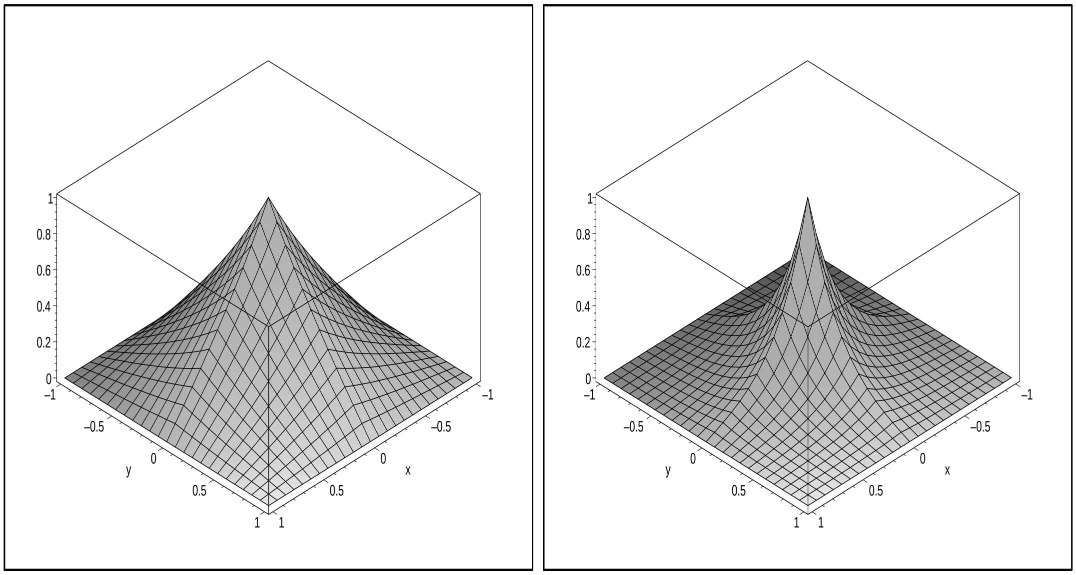

Figure 1: The function λ_k for $\varepsilon = 1$ (left) and $\varepsilon = 10^{-1}$ (right).

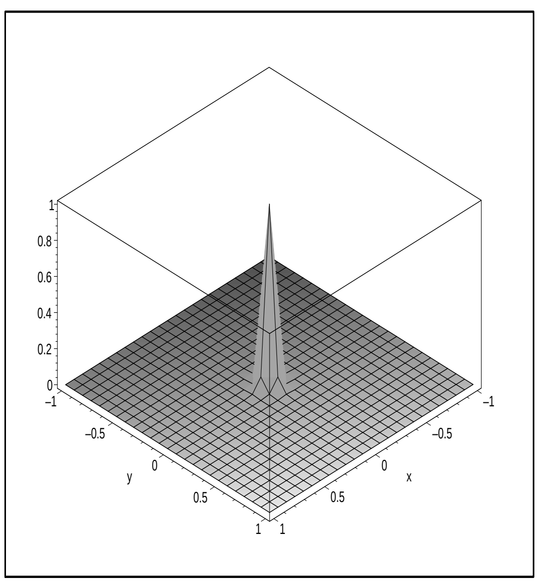

Figure 2: The function λ_k for $\varepsilon = 10^{-3}$.

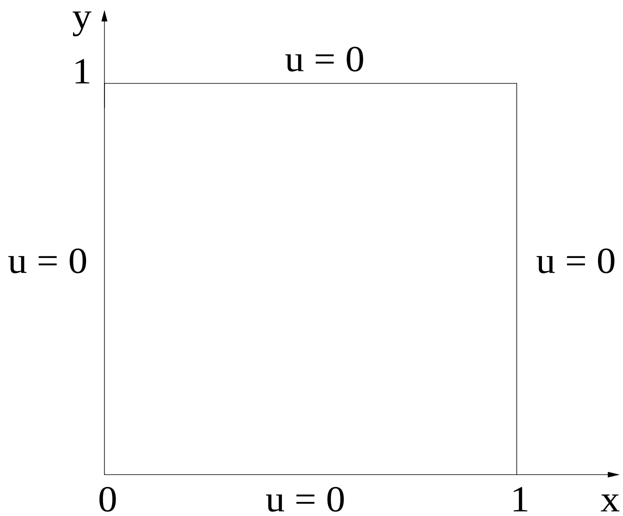

Figure 3: Problem statement.

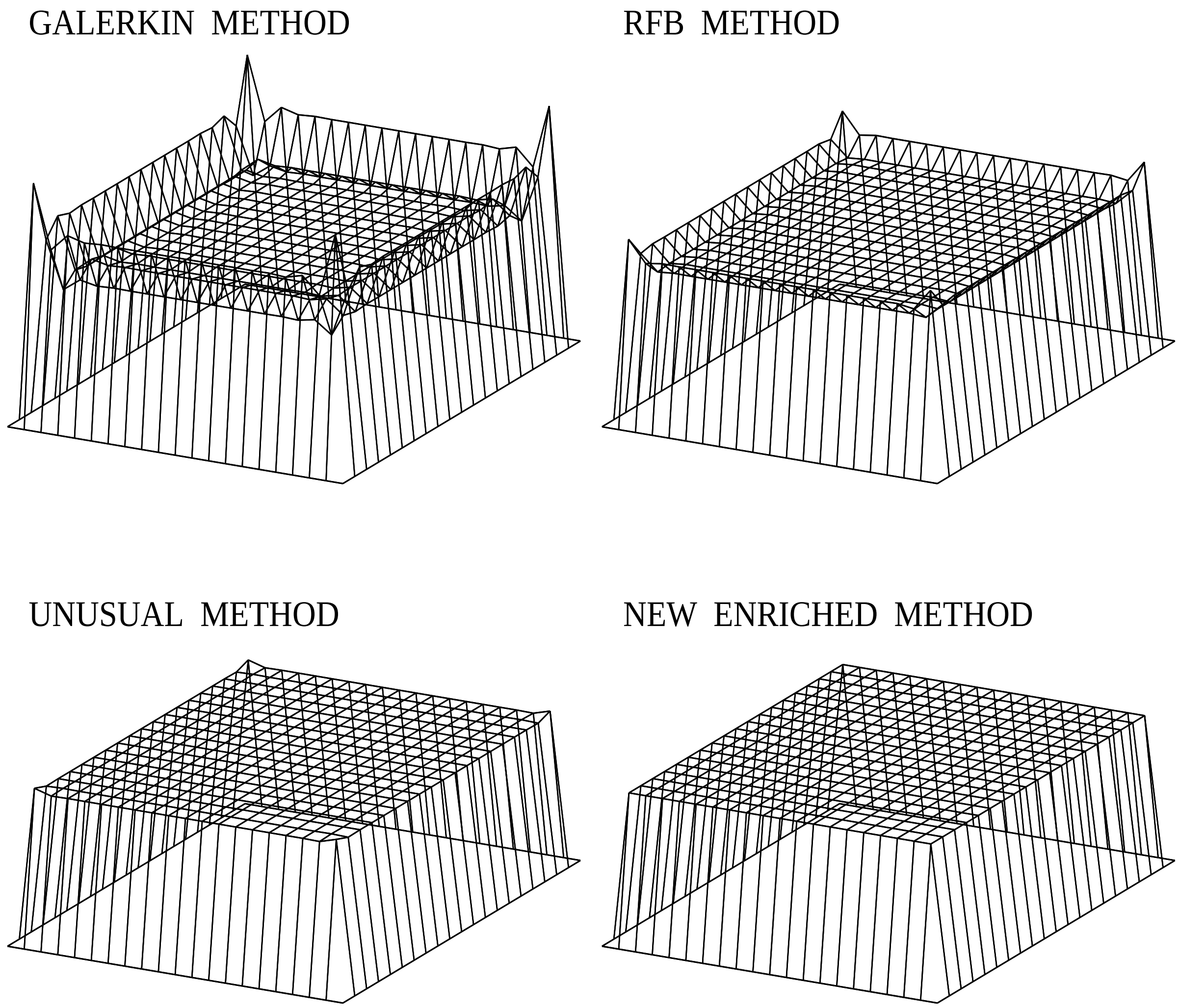

Figure 4: Comparison among Galerkin, Unusual, Residual Free Bubble, and the multiscale method for $\varepsilon = 10^{-6}$.

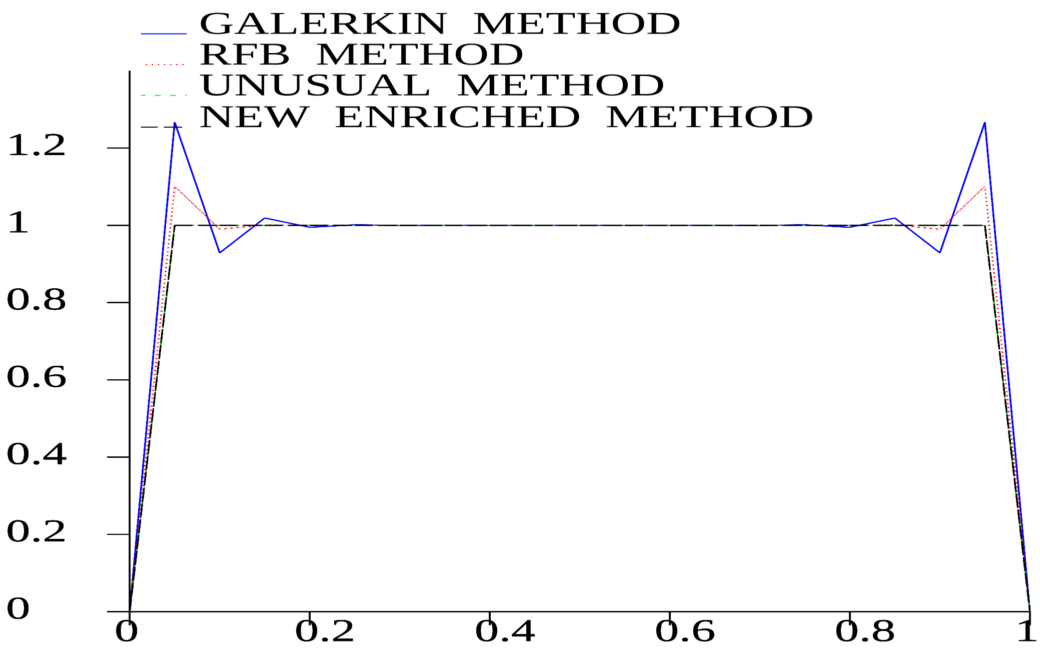

Figure 5: Profile of solutions at $x = 0.5$ ($\varepsilon = 10^{-6}$).

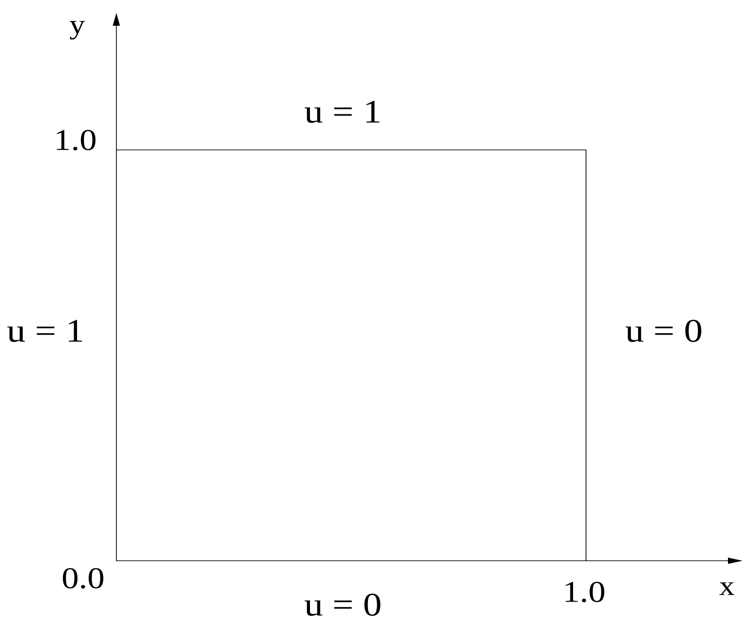

Figure 6: Problem statement.

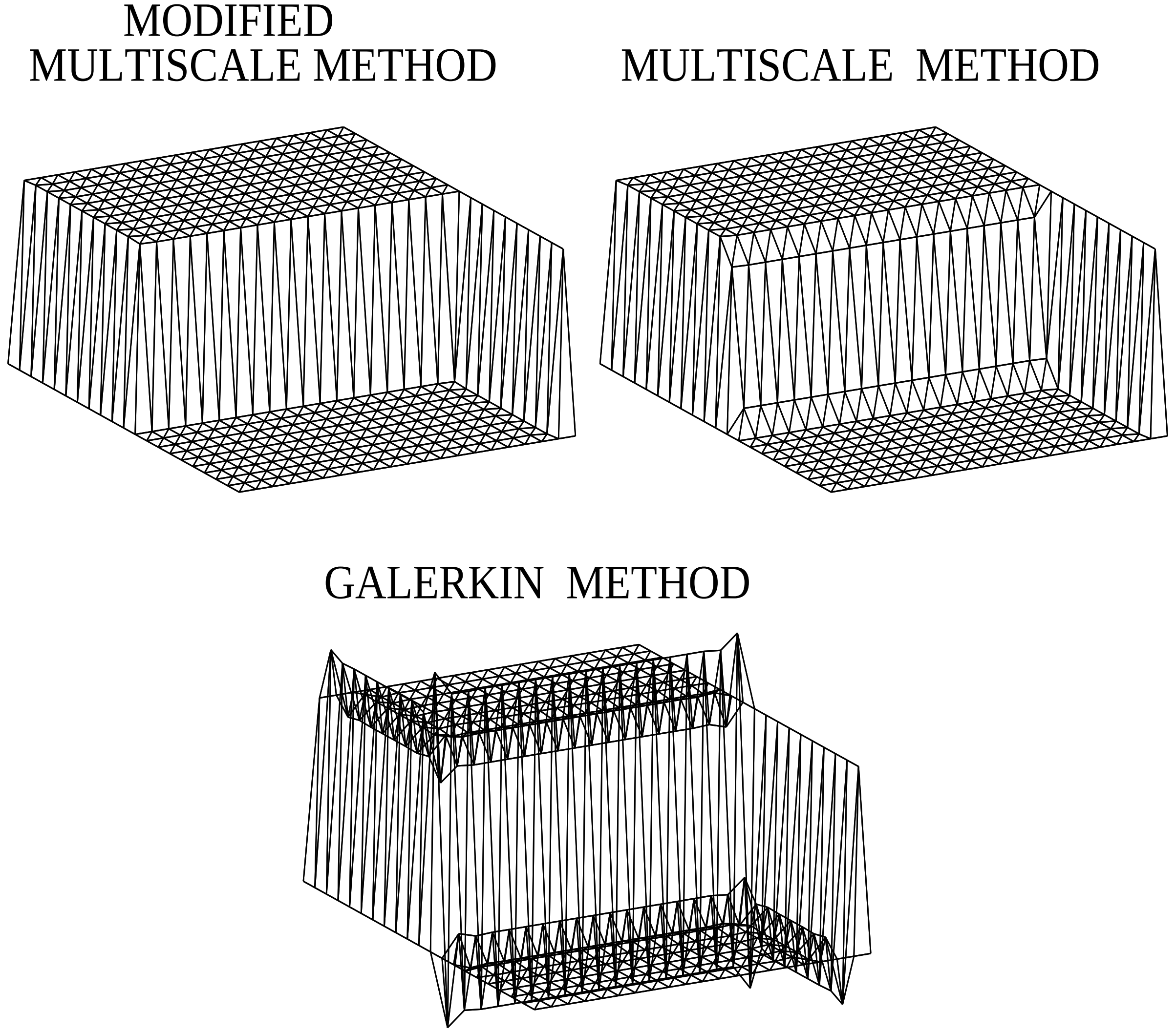

Figure 7: Comparison among Galerkin, and multiscale methods for $\varepsilon = 10^{-6}$.

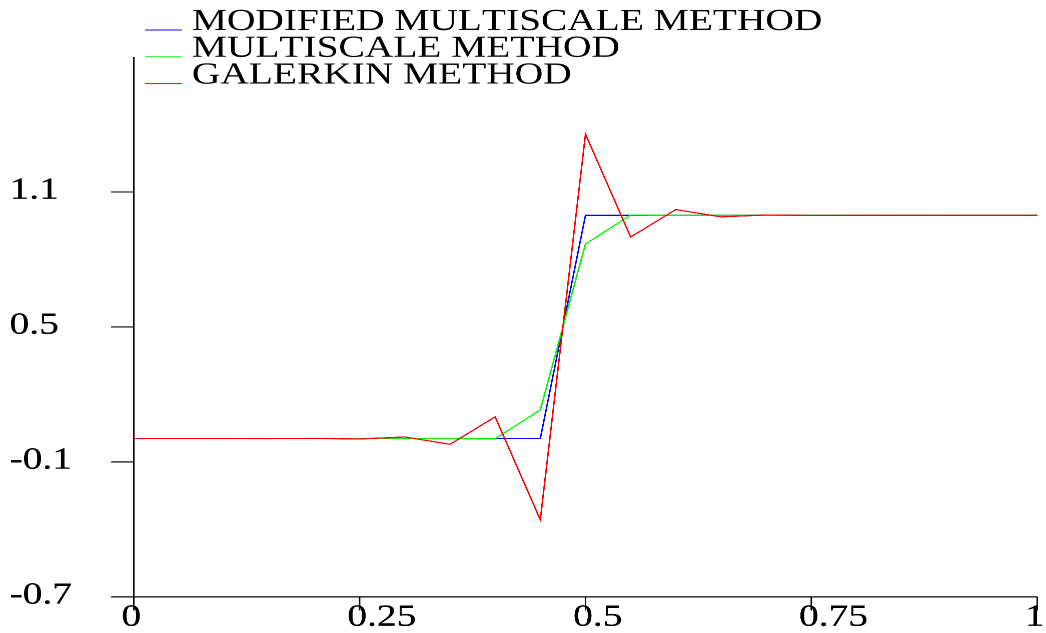

Figure 8: Profile of solutions at $x = 0.5$ ($\varepsilon = 10^{-6}$).